

The bottom of the white dwarf cooling sequence in the old open cluster NGC 2158¹

L. R. Bedin², M. Salaris³, I. R. King⁴, G. Piotto⁵, J. Anderson², and S. Cassisi⁶.

ABSTRACT

We use 10 orbits of Advanced Camera for Surveys observations to reach the end of the white dwarf cooling sequence in the solar-metallicity open cluster NGC 2158. Our photometry and completeness tests show that the end falls at magnitude $m_{F606W} = 27.5 \pm 0.15$, which implies an age between ~ 1.8 and ~ 2.0 Gyr, consistent with the age of 1.9 ± 0.2 Gyr obtained from fits to the main-sequence turn-off. The faintest white dwarfs show a clear turn toward bluer colors, as predicted by theoretical isochrones.

Subject headings: open clusters and associations: individual (NGC 2158) — Hertzsprung-Russell diagram — white dwarfs

¹ Based on observations with the NASA/ESA *Hubble Space Telescope*, obtained at the Space Telescope Science Institute, which is operated by AURA, Inc., under NASA contract NAS 5-26555, under GO-10500.

²Space Telescope Science Institute, 3800 San Martin Drive, Baltimore, MD 21218; [bedin; jayander]@stsci.edu

³Astrophysics Research Institute, Liverpool John Moores University, 12 Quays House, Birkenhead, CH41 1LD, UK; ms@astro.livjm.ac.uk

⁴Department of Astronomy, University of Washington, Box 351580, Seattle, WA 98195-1580; king@astro.washington.edu

⁵Dipartimento di Astronomia, Università di Padova, Vicolo dell'Osservatorio 2, I-35122 Padova, Italy; giampaolo.piotto@unipd.it

⁶INAF-Osservatorio Astronomico di Collurania, via M. Maggini, 64100 Teramo, Italy; cassisi@oa-teramo.inaf.it

1. Introduction

The recent discovery of an unexpectedly bright peak in the white dwarf (WD) luminosity function (LF) of the metal-rich open cluster NGC 6791 (Bedin et al. 2005a, 2008a,b) has raised questions about the physical processes that rule the formation of WDs and their cooling phases. The aim of the present work is to investigate the WD cooling sequence (CS) of another open cluster, NGC 2158, which has solar metallicity (Jacobson, Friel, & Pilachowski 2009) and is 4 times younger than NGC 6791 (Carraro et al. 2002), but somewhat less massive (as can be seen from their images in the Sky Survey). Our purpose is to extend our knowledge of the dependence of WD LFs on cluster age and metallicity.

2. Observations, Measurements, and Selections

All data were collected with the wide field channel (WFC) of the Advanced Camera for Surveys (ACS) at the focus of the *Hubble Space Telescope* (*HST*) under program GO-10500 (PI: Bedin). Data were collected between October 24, 2005, and November 9, 2006, and consist of $1 \times 0.5\text{s} + 4 \times 20\text{s} + 10 \times 1145\text{--}1150\text{s}$ images in filter F606W, and $1 \times 0.5\text{s} + 4 \times 20\text{s} + 10 \times 1130\text{--}1150\text{s}$ in F814W. Figure 1 shows a stacked image of the region that we studied, after removal of cosmic rays and most of the artifacts. To study the WDs we used only the long exposures, in which the average sky background is high enough that there are no CTE problems. The shortest exposures were used to study the brightest and evolved cluster members.

Photometry and relative positions were obtained with the software tools described by Anderson et al. (2008). In addition to solving for positions and fluxes, we also computed two important diagnostic parameters: The image-shape parameter RADXS is the fraction of light that a source has outside the predicted PSF; it is very useful for eliminating the faint blue galaxies that tend to plague studies of WDs. The sky-smoothness parameter rmsSKY is the rms deviation from the mean, for the pixels in an annulus from 3.5 to 8 pixels from each source. As discussed in Bedin et al. (2008a), rmsSKY is invaluable in measuring a more effective completeness than has been used in most previous studies.

The photometry was calibrated into the WFC/ACS Vega-mag system following the procedures given in Bedin et al. (2005b), and using encircled energy and zero points given by Sirianni et al. (2005). We will use for these calibrated magnitudes the symbols m_{F606W} and m_{F814W} .

Artificial-star (AS) tests were performed using the procedures described by Anderson et al. (2008). In the present program we chose them to cover the magnitude range $24 <$

$m_{F606W} \leq 30$, with colors that placed them on the WD sequence. These played an important role in showing us what selection criteria should be used for the real stars; the quality of our results depends very much on making a good selection, whose details are shown in Fig. 2. (See Bedin et al. 2009 for a detailed description of the selection procedures.) Panels whose labels are unprimed refer to real stars, while primed labels refer to the artificial stars.

First, we required that a star appear in at least six long exposures in each filter; panels e and e' show these selections, with the cluster center marked by a \star . Next, we used the AS to show what combinations of magnitude and RADXS are acceptable for valid star images (panel a'), and we drew the red lines to isolate the acceptable region. We then drew *these very same* lines in panel a, to separate the real stars from blends and probable galaxies. Note that the tail of objects on the right side in the AS panels is produced by star-star blends that our simultaneous-fitting routine was not able to separate into two components. These should certainly be eliminated from our photometry lists (both real and AS). We went through similar steps for the rmsSKY parameter (panels b' and b). (This step eliminated very few stars, but was quite invaluable for the completeness estimate that we are about to describe.) Finally we plotted CMDs and drew dividing lines in a similar way, to isolate the white dwarfs (panels c' and c).

Our final step was to deal with completeness, a concept that appears in two different contexts: (1) The observed numbers of stars must be corrected for a magnitude-dependent incompleteness. (2) It is customary to choose the limiting magnitude at the level where the sample is 50% complete. In a star cluster these two aims need to be treated in quite different ways. (1) To correct for incompleteness, we use the traditional ratio of AS recovered to the number inserted. (2) For the limit to which measures of faint stars are reliable, however, the 50%-completeness level needs to be chosen in a quite different way, because in a crowded star cluster more faint stars are lost in the brightness fluctuations around the bright stars than are lost to the fluctuations of the sky background. The completeness measure that we should use to set the 50% limit is therefore the recovered fraction of AS *only* among those AS whose value of rmsSKY, as a function of magnitude, indicates that it *was possible to recover the star at all*. [For a more detailed discussion, see Sect. 4 of Bedin et al. (2008a)].

The distinction between the two completeness measures is illustrated in panel d of Fig. 2, where the black crosses and line show the overall completeness, while the blue squares and line show the completeness statistic that takes rmsSKY into account; its 50% completeness level is at $m_{F606W} = 28.95$, rather than the 28.26 with which the traditional statistic would have left us. To emphasize the contrast, the red circles and line show the fraction of the area in which faint stars could have been found at all.

3. Comparison with Theory

The comparison with theory has three parts: (a) determination of a main-sequence (MS) turn-off (TO) age, (b) comparison between the observed WD sequence and theoretical isochrones, and (c) determination of the age that is implied by the WD LF.

For the fitting of the MSTO we used the BaSTI scaled-solar models and isochrones, including convective-core overshooting (Pietrinferni et al. 2004), but we needed first to choose a value of the metallicity. The literature of NGC 2158 had offered a wide range of $[\text{Fe}/\text{H}]$ values (~ -0.2 to ~ -0.9) and of $E(B - V)$ (~ 0.4 to ~ 0.6), as recently summarized by Jacobson et al. (2009). Those authors presented the first high-resolution spectroscopic analysis of NGC 2158, and arrived at $[\text{Fe}/\text{H}] = -0.03 \pm 0.14$. From a cubic interpolation among the isochrones in the BaSTI database, we derived scaled-solar isochrones for that $[\text{Fe}/\text{H}]$ value, and determined the cluster reddening and distance modulus, as follows. We first allowed for the effect of extinction, as described by Bedin et al. (2009) for the globular cluster M4, and we then estimated the distance modulus, reddening, and age of the cluster by matching isochrones simultaneously to the mean color and magnitude of the red clump (to fix distance and extinction — see the box in Fig. 3) and to the location of the TO region (to fix the age).

The upper-right panel of Fig. 3 shows isochrones that bracket the observed TO luminosity, two with overshooting and two without. It is clear that no good fit to the MSTO region can be obtained without overshooting. The isochrones that fit the red clump and the MSTO also give a good fit to the MS. For $[\text{Fe}/\text{H}] = -0.03$ we obtain $A_V = 1.3$ [corresponding to $E(B - V) = 0.42$], $(m - M)_0 = 12.98$, and an age between 1.75 and 2.0 Gyr. This age is consistent with previous results by Carraro et al. (2002) and Salaris et al. (2004) with different methods, models, and $[\text{Fe}/\text{H}]$, while the values of reddening and distance modulus agree with results by Grocholski & Sarajedini (2002) based on a study of the red clump in the K vs. $(J - K)$ CMD.

To estimate the error in the fit of the sparsely populated red clump (only 12 stars), we synthesized from each isochrone a rich CMD of this region (several thousand stars), and compared these theoretical representations of the red clump with the observed one. The $1\text{-}\sigma$ spreads in the fit are ± 0.05 mag in the mean m_{F606W} , and ± 0.02 mag in the mean color.

A total uncertainty of ± 0.06 mag for $(m - M)_0$ has been estimated by adding in quadrature the ± 0.05 mag uncertainty in the mean m_{F606W} of the observed red clump, and a ± 0.03 mag contribution due to the change of the mean m_{F606W} of the isochrone red clump when $[\text{Fe}/\text{H}]$ is changed by its ± 0.14 dex uncertainty. (We did this for a fixed age of 2 Gyr; the mean magnitude of the isochrone red clump changes negligibly for age changes of a few hundred Myr around that value.)

To estimate the error in A_V , we first added in quadrature the ± 0.02 mag uncertainty in the mean color of the observed red clump, and a ± 0.03 mag uncertainty in the mean color of the isochrone red clump, the latter corresponding to the uncertainty in $[\text{Fe}/\text{H}]$. The combined color uncertainty was then converted to a ± 0.09 mag uncertainty in A_V , by using the Cardelli et al. (1989) extinction law, with $R_V = 3.1$.

As for the age, we estimated its total uncertainty by adding four separate contributions in quadrature: first a ± 0.125 Gyr uncertainty in the fit itself, even at fixed values of $[\text{Fe}/\text{H}]$, distance, and extinction, and then contributions from allowing each one of those three to vary while holding the other two constant — ± 0.08 Gyr from $[\text{Fe}/\text{H}]$, ± 0.06 Gyr from the distance modulus, and ± 0.08 Gyr from the extinction. Our final value of the MSTO age is 1.9 ± 0.2 Gyr.

We move now to the white dwarfs. For them we found it preferable to work with different data samples for the shape of the WD CS and for the WD LF. The best WD CMD came from a radial selection (blue circle in Fig. 2) that excludes the crowded cluster center; this leads to a cleaner WD sequence for the comparison with isochrones (top-left panel of Fig. 3). Such a selection, however, would drastically reduce in the numbers of stars in our WD LF, where narrowing of the sequence is of no benefit; we therefore used the entire sample (shown in panel c of Fig. 2) for the fitting of the LF.

One more point to note is that in the LF we concentrate only on the peak at the faint end, because dynamical evolution in the cluster has distorted the detailed shape of the LF in a way that is too complicated to model. This is suggested by the binary sequence that can be seen to the right of the MS, also in panel c of Fig. 2. Unlike the smooth distribution of binaries that is seen in many globular clusters, the binary sequence here is sharply peaked at the red edge that corresponds to equal-mass binaries. Binaries of unequal mass ratio have a lower mass than those of equal mass, and have been largely removed by the mass-dependent escape of stars. The effect on the WD LF is very hard to estimate in detail, but there is no effect on the location of the peak at the faint end, which is what we use for estimating the cluster age.

For WD theory we used the carbon-oxygen WD models by Salaris et al. (2000), transformed into the ACS Vega-mag system as described in Bedin et al. (2005a,b). The top left panel of Fig. 3 compares WD isochrones with the observed WD sequence. We used isochrones from our H-atmosphere WD models, along with the initial-final-mass relationship by Salaris et al. (2009), and the progenitor lifetimes for $[\text{Fe}/\text{H}] = -0.03$, obtained again by interpolation among the values from the BaSTI database. Isochrones for 1.75 and 2.0 Gyr are overplotted on the observed WD sequence, using our derived values $A_V = 1.3$ and $(m - M)_0 = 12.98$. In the more vertical part of the WD sequence, where the errors are small,

they fit well, and they turn to the blue at the right magnitude.

The WD cooling track for a $0.61 M_{\odot}$ WD with He envelope is also shown. Its mass is close to the mass ($\sim 0.65 M_{\odot}$) of objects evolving along the bright linear part of the H-atmosphere WD isochrone, and we take it as representative of the non-DA population that may possibly contaminate the observed cooling sequence.

We also show the cooling track of the $0.465 M_{\odot}$ He-core WDs that we used in our previous work on NGC 6791 (Bedin et al. 2008a) to estimate the location of He-core WDs — if they exist in the cluster — compared with the CO-core sequence. The maximum electron-degenerate He-core mass for NGC 2158 stars is $\sim 0.45 M_{\odot}$ for the objects currently at the tip of the red giant branch (total masses of the order of $1.7\text{--}1.8 M_{\odot}$); therefore the He-core WDs — in the absence of episodes of mass accretion from He-core WD companions — have to populate a CMD region to the red of the $0.465 M_{\odot}$ model that is shown. We conclude from Fig. 3 that the contamination of the observed cooling sequence by He-core WDs has to be negligible.

The lower panel of Fig. 3 compares the observed WD LF in F606W with theory. The observed sample contains 138 WD candidates, which become 183 after correction for incompleteness. We show the two ages, 1.75 and 2.0 Gyr, that bracket the MSTO age. Our theoretical LFs come from H-atmosphere WD isochrones that were produced by using a Monte Carlo method to synthesize a WD sequence, as described in Bedin et al. (2008b). The simulations minimize the effect of random fluctuations of star counts, by using ~ 1000 times as many WDs as the observed sequence, and include appropriate photometric errors as found from the data-reduction procedure. We used a Salpeter mass function for the WD progenitors, and included the effect of incompleteness by randomly removing stars according to the completeness curves described in Section 2.

Given the presence of a clear binary sequence that parallels the the MS, we included in our synthetic WD sequences a 20% fraction of unresolved WD+WD binary systems. (See Bedin et al. 2008b for details.). Neither the inclusion of WD+WD binaries nor the precise choice of the progenitor mass function affects the position of the LF cutoff for a given age. For the plots of Fig. 3 the total number of stars in the synthetic WD sequences has been rescaled to match the observed number of objects in the magnitude interval $24.5 \leq m_{\text{F606W}} \leq 26.0$.

The observed and theoretical LFs are clearly consistent. In particular, if we locate the cut-off of the observed LF at the magnitude of the faintest bin whose star counts are above zero by 3σ ($m_{\text{F606W}} = 27.500 \pm 0.125$), the two LFs for 1.75 and 2.0 Gyr represent lower and upper limits for the age inferred from the WDs, in nice agreement with the result from the MSTO. We note also that the uncertainties in the distance modulus and in the metallicity

of the progenitors have a negligible effect ($\sim \pm 50$ Myr) on this age range.

The overall shapes of the observed LFs in both filters are very similar to their theoretical counterparts, but we refrain at this stage from attempting a more quantitative fit (or even a bi-dimensional fit of the WD distribution in the CMD) for several reasons: The exact shape of the WD LF (and of the WD sequence in the CMD) depends on a number of parameters in addition to the cluster age, e.g., the initial-final-mass relationship, the mass function of the progenitors, the relative fraction of H- and He-atmosphere objects, the fraction of WD+WD binaries (and their mass distribution) and, very importantly (as explained earlier in this section), dynamical evolution of the cluster, which selectively depletes the WDs according to their mass and their time of formation. The observed position of the LF cut-off, however, which determines our WD age, should have been affected very little, if at all, by the dynamics of the cluster, for the following reason. The WD isochrones predict that for ages around the MSTO age, the brighter WDs should have nearly a single mass, whereas the 0.25-mag bin at the LF cutoff — i.e., at the blue-turn at the bottom of the CS — should be populated by objects spanning almost the whole predicted WD mass spectrum. A mass-dependent loss mechanism would therefore alter the number distribution of WDs around the blue-turn, but it should have no effect on the observed location of the cut-off in the WD LF.

We close this section by addressing briefly the issue of WDs that have an atmosphere of helium rather than hydrogen. For the temperature range of the NGC 2158 cooling sequence, the typical number ratio of He- to H-atmosphere WDs in the field is of the order of 1:4 (e.g., Tremblay & Bergeron 2008), but it is not clear whether there is a dearth of He-atmosphere WDs in star clusters compared to the field (see, e.g., Strickler et al. 2009, Davis et al. 2009). In spite of this uncertainty, at the luminosities of the NGC 2158 WDs the He-atmosphere models have cooling ages very similar to those of H-atmosphere models at the same mass (see, e.g., Hansen 1999, Salaris 2009). If the observed cooling sequence includes He-atmosphere WDs, even in substantial number, their effect on the ages estimated from the position of the LF cutoff would be negligible.

We warmly thank an anonymous referee for useful comments. J.A. and I.R.K. acknowledge support from STScI grant GO-10500. GP acknowledges support by PRIN2007 and ASI under the program ASI-INAF I/016/07/0.

REFERENCES

Anderson, J., et al. 2008, *AJ*, 135, 2055

- Bedin, L. R., Salaris, M., Piotto, G., King, I. R., Anderson, J., Cassisi, S., & Momany, Y. 2005a, *ApJ*, 624, L45
- Bedin, L. R., Cassisi, S., Castelli, F., Piotto, G., Anderson, J., Salaris, M., Momany, Y., & Pietrinferni, A. 2005b, *MNRAS*, 357, 1038
- Bedin, L. R., King, I. R., Anderson, J., Piotto, G., Salaris, M., Cassisi, S., & Serenelli, A. 2008a, *ApJ*, 678, 1279
- Bedin, L. R., Salaris, M., Piotto, G., Cassisi, S., Milone, A. P., Anderson, J., & King, I. R. 2008b, *ApJ*, 679, L29
- Bedin, L. R., Salaris, M., Piotto, G., Anderson, J., King, I. R., & Cassisi, S. 2009, *ApJ*, 697, 965
- Carraro, G., & Girardi, L., Marigo, P. 2002 *MNRAS*, 332, 705
- Grocholski, A. J., & Sarajedini, A. 2002, *AJ*, 123, 1603
- Hansen, B. M. S. 1999, *ApJ*, 520, 680
- Jacobson, H. R., Friel, E. D., & Pilachowski, C. A. 2009, *AJ*, 137, 4753
- Pietrinferni, A., Cassisi, S., Salaris, M., & Castelli, F. 2004, *ApJ*, 612, 168
- Salaris, M., García-Berro, E., Hernanz, M., Isern, J., & Saumon, D. *ApJ*, 2000, 544, 1036
- Salaris, M., Weiss, A., & Percival, S. M. 2004, *A&A*, 414, 163
- Salaris, M., Serenelli, A., Weiss, A., & Miller Bertolami, M., 2009, *ApJ*, 692, 1013
- Salaris, M. 2009, in “The Ages of Stars”, *Proceedings of the International Astronomical Union, IAU Sym.*, v. 258, p. 287
- Davis, D. S., et al. 2009, *ApJ*, in press (2009arXiv0909.2254S)
- Sirianni, M., et al. 2005, *PASP*, 117, 1049
- Strickler, R. R., Cool, A. M., Anderson, J., Cohn, H. N., Lugger, P. M., & Serenelli, A. M. 2009, *ApJ*, 699, 40
- Tremblay, P. E. & Bergeron, P. 2008, *ApJ*, 672, 1144

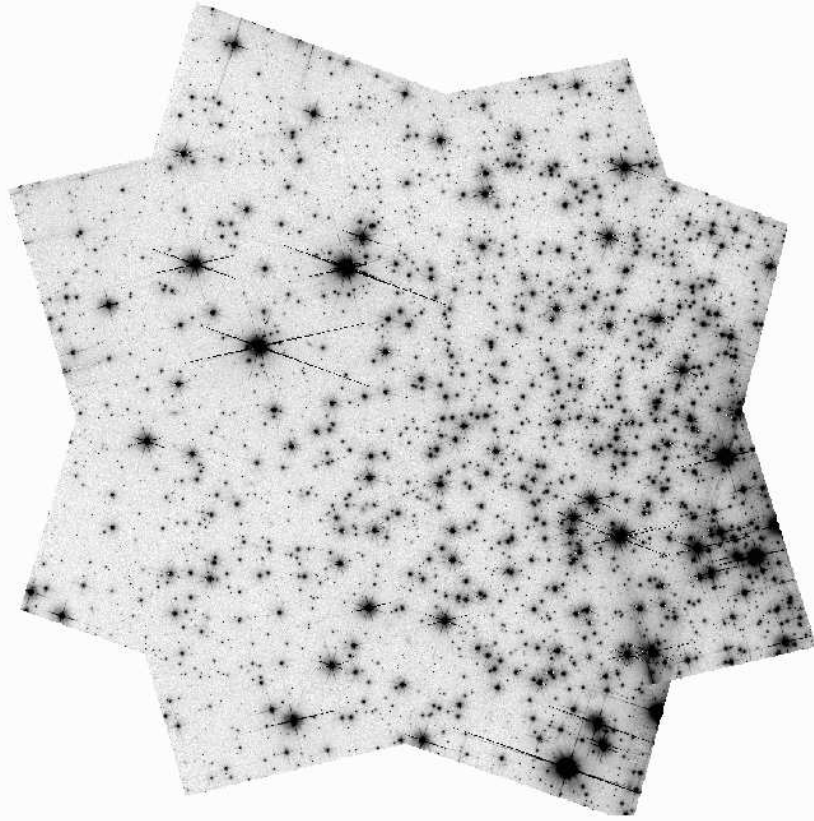


Fig. 1.— Stacked image of deep exposures in filter F814W.

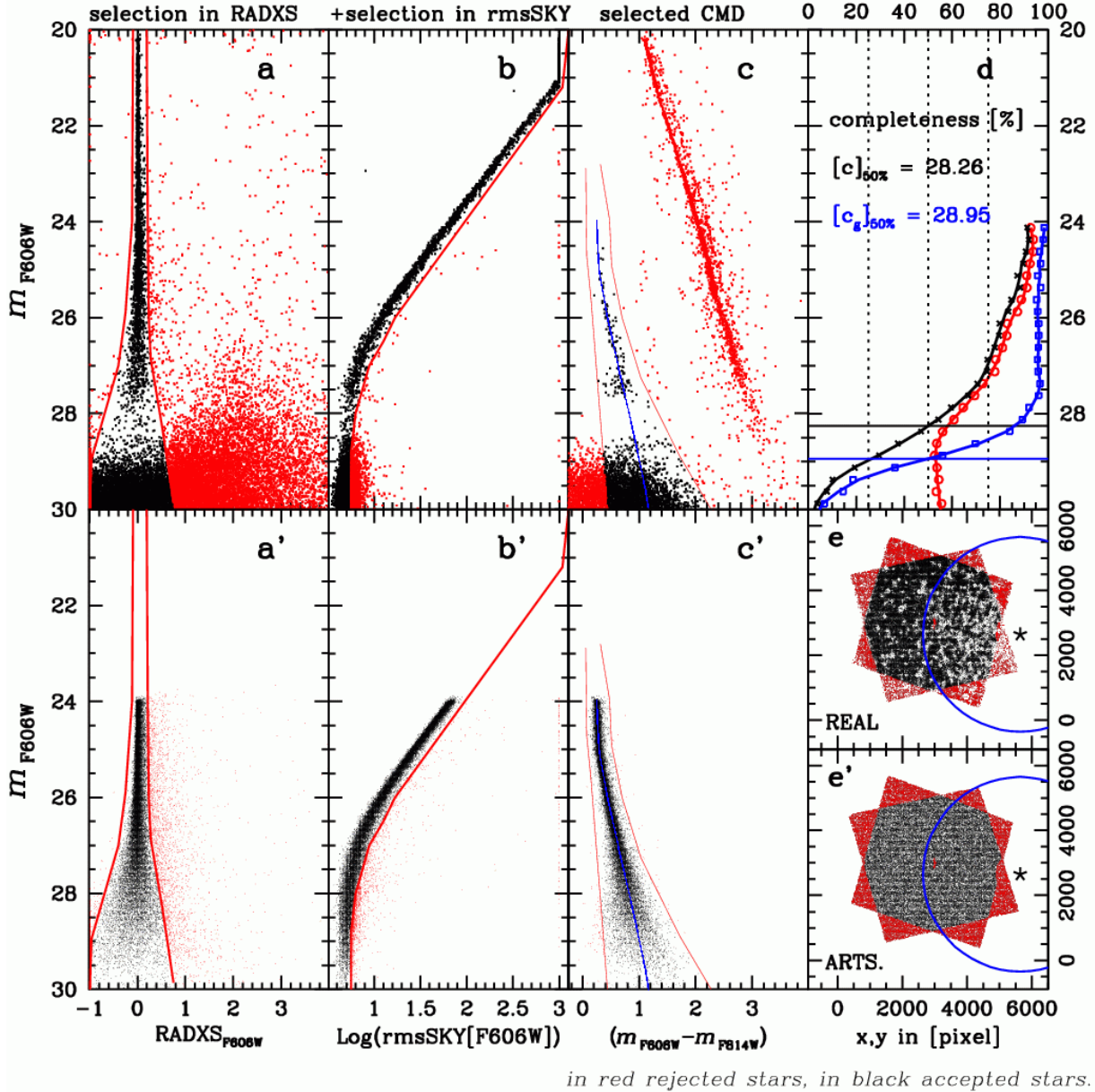


Fig. 2.— (a) and (a’): The parameter RADXS as a function of magnitude, for real stars and AS. Objects that we consider to be real stars lie between the two red lines. (b) and (b’): The parameter rmsSKY as a function of magnitude. Stars that lie on an acceptable background lie to the left of the red line. (c) and (c’): The CMD, with red lines delineating the WD region. The blue lines show the fiducial line along which the AS were added. (d): Black points and line show the traditional “completeness” that ignores the rmsSKY criterion, while the blue points and line show the completeness in the regions in which faint stars can be detected and measured. The red circles and line show the fraction of the total that this measurable area comprises. Panels (e) and (e’): Spatial distribution of the real and AS detections. In black, objects that fell in at least 6 deep images in both F606W and F814W. The assumed cluster center is marked with a \star . The blue circles identify the radius outside of which the more restricted WD sample was taken (see Sect. 3).

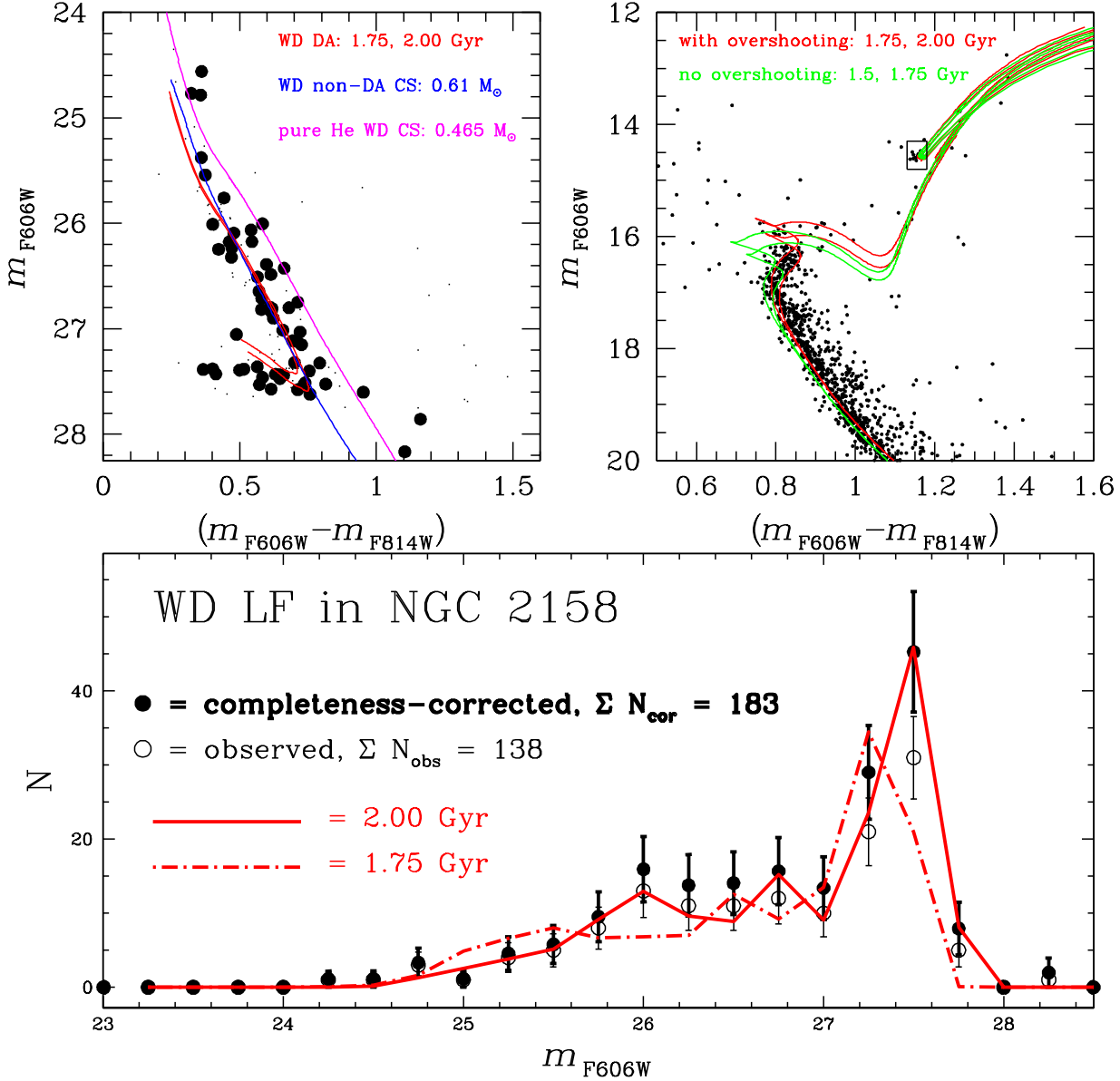


Fig. 3.— (*upper left:*) The observed cooling sequence compared to theoretical H-atmosphere WD isochrones (red lines) for 1.75 and 2.0 Gyr, shifted in color and magnitude according to the distance modulus and extinction estimated from fits to the MS, its TO, and the red clump. The blue line is the cooling track of a $0.61M_{\odot}$ He-atmosphere WD, while the magenta line represents a $0.465M_{\odot}$ He-core WD. (*upper right:*) Fit of theoretical isochrones to the cluster CMD, from the MS to the red clump, for ages of 1.75 and 2.0 Gyr. (*bottom:*) comparison between the observed WD LF in F606W and its theoretical counterpart, for 1.75 and 2.0 Gyr. (See text for details).

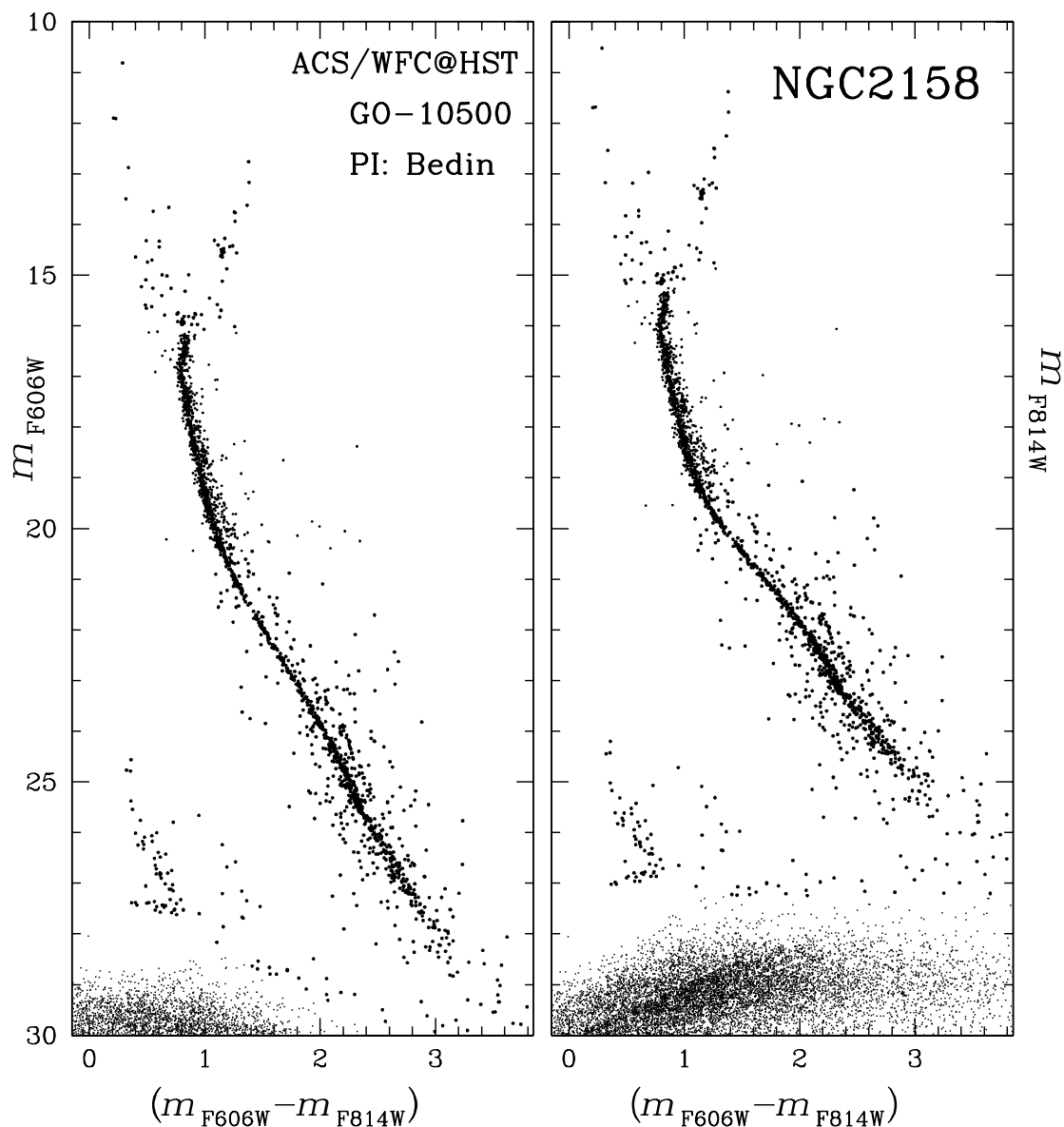


Fig. 4.— **(Bonus-material only for the astro-ph version of the draft):** The two panels show the entire CMDs, obtained including short-, middle- and long-exposures. Note that photometries derived from images of different exposure times are subject to different selections. Objects measured in the short (0.5 s) and long (1200 s) exposures are marked with larger filled circles than those measured in middle exposures. Small dots are considered non-significant detections and indicate the floor-noise level in the background.